Hydrodynamic Focusing of Particle Trajectories in Light-Scattering Counters and Phase-Doppler Analysers

Vladimir I. Ovod*

(Received: 3 May 1994; resubmitted: 10 April 1995)

Abstract

To reduce errors when measuring sizes of particles in light-scattering counters and phase-Doppler analysers, the hydrodynamic focusing of particle trajectories in relation to the centre of the measurement zone is used. This focusing is effected in a special running-type chamber. Equations describing the mechanical energy of liquid flows running through a running-type chamber have been compiled. By solving a system of such equations, relatively simple equations for engineering calculations of the coefficient of hydrodynamic compression of particle trajectories in relation to the centre of the measurement zone have been obtained. Results of experimental research are given and the application of the proposed technique for designing improved running-type chambers with one and two „sheaths" is demonstrated.

1 Introduction

Proximate single-particle size analysers are built on the basis of measuring parameters (amplitude [1–3], energy [4, 5], duration [6] or phase [7–9]) of light pulses. These pulses are generated in the analyser owing to scattering of laser radiation on single particles which cross the focused laser in the measurement zone. The problems of designing particle laser analysers and their application in industry, medicine and ecology have been discussed by numerous workers [1–11]. It has been found that the accuracy of measuring particles depends considerably on the coincidence of particle trajectories with the centre of the measurement zone [4, 6, 8, 9]. Inaccuracy is caused by irregularity in the spatial distribution of laser radiation in the measurement zone. The most effective means of reducing the deflection of particle trajectories is the hydrodynamic focusing of particle trajectories in a special chamber of the running type. In this case, a liquid is used as the transportation medium. The liquid makes it possible, as *Steinkamp* et al. demonstrated [4, 10], to carry out life analysis of biological cells, destroy aggregates of particles and sort out particles according to their sizes. Some workers, such as *Kachel* [14], *Gransson* [15] and *Merkus* et al. [16], investigated the question of hydrodynamic focusing of particles aimed at increasing the measurement accuracy in devices which are based on the Coulter principle (principle of electrical resistance measurement in the sensitive zone of the orifice). Other publications [4, 5, 10, 12, 13] concerning the questions of hydrodynamic focusing of particles in laser analysers have, in general, a descriptive character in relation to the construction of a running-type chamber. This descriptive approach makes the development of particle analysers with improved metrological characteristics more difficult.

This paper deals with the analysis of hydrodynamic focusing of particle trajectories in a running-type chamber in relation to the centre of the laser analyser's measurement zone. Equations convenient for the engineering calculations of chamber parameters have been obtained, and experimental data are presented.

2 Efficiency of Hydrodynamic Focusing of Particle Flow

Figure 1 shows a generalized diagram of the running-type chamber of the laser analysers.

A capillary 1 with the area of internal section S_c and length l_c, a pipe 3 and an output nozzle (or opening) 6 are aligned. The suspension with particles 2 being measured enters the running-type chamber through capillary 1 under pressure P_o. The pipe 3 with cross-sectional area S_{pl} below the plane (I) takes the shape of the conical (conoidal) nozzle 4, with the smallest sec-

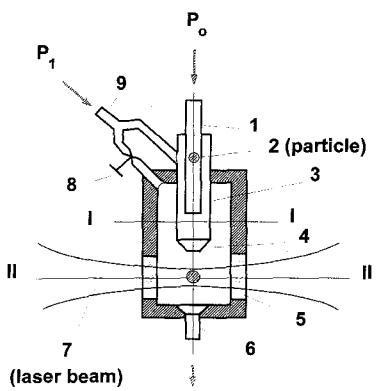

Fig. 1: Generalized diagram of the running-type chamber for hydrodynamic focusing of a flow of particles being examined with liquid of two buffer "sheaths": 1 = capillary; 2 = particle; 3 = pipe; 4 = nozzle; 5 = transparent windows (dish); 6 = output nozzle; 7 = laser beam; 8 = tap; 9 = inlet for injecting liquid of sheath.

* Dr. *V. I. Ovod*, Universität Bremen, Verfahrenstechnik/FB 4, Badgasteinerstr. 3, 28359 Bremen (Germany). On leave from the Optical Engineering Department, Kiev Polytechnical Institute, Brest-Litovsky prosp. 37, 252056 Kiev (Ukraine).

0934-0866/95/0408-0207 $5.00 + .25/0

tion of the narrow zone having an area S_{p2}. The body of the running-type chamber 5 is made of a material transparent to a laser beam 7. This beam enters the plane (II) and is focused in the zone where it crosses the particle flow (the measurement zone).

To reduce the probability of clogging the internal channels of the running-type chamber, the minimal lateral sizes of the capillary 1 and the nozzle 4 are usually larger than 200 μm. The deviation of particle trajectories from the centre of the measurement zone is reduced by the hydrodynamic compression of the flow of suspension being examined down to a diameter commensurate with the maximum dimensions of the particles to be examined. This compression is effected by means of a liquid of the so-called first "sheath" at the combined outflow of this liquid with the suspension being examined from the converging nozzle 4 into the chamber 5. The first "sheath" passes under pressure P_1 into the pipe 3 through an inlet 9. The chamber 5 is filled with liquid of the second sheath, and prevents the formation of surface waves and other phenomena on the border of the phase separation, which can be a source of parasitic scattering of the laser radiation.

As shown in Figure 2, the criterion of efficiency of the hydrodynamic focusing of the particle flow in the compression coefficient is calculated by the equation

$$k = \frac{S_c}{S_{m2}}, \tag{1}$$

where $S_{m2} = \pi r_{m2}^2$ is the area of the cross-section of the suspension flow being examined in plane II.

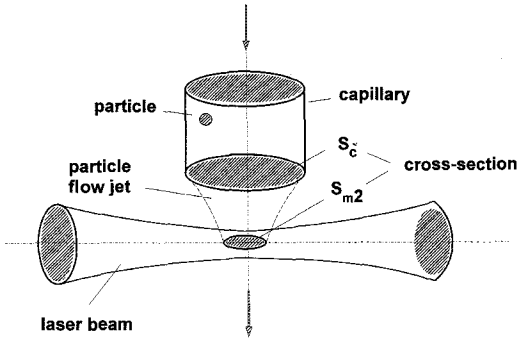

Fig. 2: Principle of the hydrodynamic focusing, supplying the given coefficient value $k = S_c/S_{m2}$ of hydrodynamic compression of particle flow jet from cross-section S_c in the capillary area to cross-section S_{m2} in the measurement zone.

The value of the coefficient k may be adjusted by changing the ratio of the flow rates of the first Q_f and second Q_s sheaths with a tap 8 (see Figure 1) or with the pressure P_o changing the flow rate Q_m of the examined suspension. In one particular case, the running-type chamber, as shown in Figure 3, may be manufactured without the second sheath.

With more complicated manufacturing technology of the running-type chamber, we can draw together the internal walls of the chamber 5 until we obtain a square-shaped channel of small size with an area of internal section S_{p2}. Lateral sections (I) and (II) are located at distances exceeding 0.035 R Re from the inputs and outputs of the channels (where R is the hydraulic radius of the channel and Re is the Reynolds number), so that the end effects are appreciably small [17].

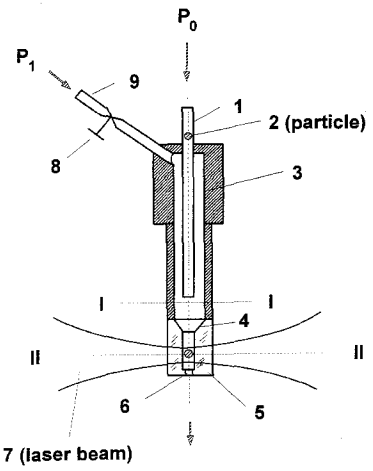

Fig. 3: Diagram of the one-sheath running-type chamber for hydrodynamic focusing of a flow of examined particles. Designations as in Figure 1.

It must also be noted that under conditions of operation, the running-type chamber may be related to isomeric systems with uncompressed, Newtonian liquids, and since the concentrations and particle sizes in the suspension being examined are so small, they do not essentially influence the balance of mechanical energy of the running-type system and they do not affect the density of the suspension being examined, which is equal to the density of the liquids of the first and second sheaths.

With due consideration of the above, we may present the balance of the mechanical energy for the liquid being examined and located between planes (I) and (II) in the form

$$2\frac{P_1 - P_2}{\gamma} + 2g(h_1 - h_2) = a_{m2} V_{m2}^2 - a_{m1} V_{m1}^2 + \sum_i (\xi_{ri} V_{mi}^2) + \sum_j (\xi_{lj} V_{mj}^2) + \sum_k (\xi_{ek} V_{mk}^2), \tag{2}$$

where P_1, P_2 are the hydrodynamic pressures, a_{m1}, a_{m2} are the Coriolis coefficients for the suspension being examined, V_{m1}, V_{m2} are the average velocities of the above-mentioned suspension in planes (I) and (II), h_1, h_2 are the distances to these planes from an arbitrarily selected horizontal plane of comparison, γ is the specific gravity of the liquid, g is the acceleration due to gravity, ξ_{ri} is the coefficient of pressure losses at the ith obstacle (fitting, etc.), V_{mi} is the average velocity of the suspension being examined in the flow section located further downstream than the ith obstacle, and ξ_{lj} and V_{mj} are the coefficient of pressure losses over the length and the average velocity at the jth straight path. The coefficient of pressure ξ_{ek} shows what part of the kinetic energy of the suspension being examined is given away (positive coefficient) via the border of separation of flows at the kth path to the liquid of the first sheath surrounding it, or, vice versa, has been obtained (negative) from the first sheath.

The Coriolis coefficient in the jth section a_j, representing the ratio of efficient kinetic energy of the flow (determined on the basis of local velocities in this section) to kinetic energy (calculated on the basis of average velocity of flow in this section), when there are no end effects, may be determined by the equation

$$a_j = \frac{1}{V_j S} \int_s V_j \, dS, \tag{3}$$

where V_j is the velocity distribution in the jth section. The integration is carried out over all the area of the jth section.
We will now write average velocities of the suspension being examined in terms of flow rate Q_m: $V_{mi} = Q_m/(\varepsilon_i S_{m2})$, where $\varepsilon_i = S_{mi}/S_{m2}$ (S_{mi} is the cross-sectional area of the flow of suspension being examined in the ith path), and transform Eq. (1) into the form

$$2\frac{P_1 - P_2}{\gamma} + 2g(h_1 - h_2) = Q_m^2\left(\frac{1}{\varphi_m^2 S_{m2}} - \frac{a_{m1}}{\varepsilon_c^2 S_c^2}\right), \quad (4)$$

where $\varepsilon_c = S_{m1}/S_c$ is the comparison coefficient of the capillary 1,

$$\varphi_m = \frac{\varphi_{rm}\varphi_{em}}{\sqrt{(1-\varphi_{rm}^2)\varphi_{em}^2 + \varphi_{rm}^2}} \quad (5)$$

is the coefficient of the velocity of the suspension being examined, taking into account all the losses in the path between planes (I) and (II),

$$\varphi_{rm} = \frac{1}{\sqrt{a_{m2} + \sum_j\left(\frac{\xi_{lj}}{\varepsilon_j}\right) + \sum_i\left(\frac{\xi_{ri}}{\varepsilon_i}\right)}} \quad (6)$$

is the component of the velocity coefficient taking into account only the friction losses along the length and losses at obstacles, and

$$\varphi_{em} = \frac{1}{\sqrt{1 + \sum_k\left(\frac{\xi_{ek}}{\varepsilon_k}\right)}} \quad (7)$$

is the component of the velocity coefficient taking into account the transfer of kinetic energy via the border of flow separation (the first term shows that in the path of energy transfer the Coriolis coefficient is close to 1 owing to of levelling of the velocity profile).
The balance of mechanical energy of the first sheath of liquid enclosed between planes (I) and (II), after transformations similar to those carried out above and ignoring the kinetic energy of the first sheath in plane (I), may be presented as

$$\frac{P_1 - P_2}{\gamma} + g(h_1 - h_2) = \frac{Q_f^2}{2\varepsilon_n^2\varphi_f^2 S_{f2}^2}, \quad (8)$$

where ε_n is the compression coefficient of the nozzle 4, φ_f is the coefficient of the first envelope velocity calculated by equations similar to Eqs. (5)–(7) and $S_{f2} = S_{p2} - S_{m2}$ is the area of the flow lateral section of the first sheath in section (II).
Solving the system of Eqs. (4) and (8) and carrying out simple transformations, we obtain the dependence of the flow compression coefficient of the suspension being examined upon design parameters of the running-type chamber:

$$(\chi k - 1)^2\left(\frac{1}{\varphi_m^2} - \frac{a_{m1}}{\varepsilon_{m1}^2 k^2}\right) = \left(\frac{Q_f}{Q_m\varepsilon_n\varphi_f}\right)^2, \quad (9)$$

where $\chi = S_{p2}/S_c$. At $k \gg 4$, the following equation may be used in engineering calculations:

$$k = \frac{Q_f}{Q_m}\left(\frac{\varphi_m}{\mu_f\chi}\right), \quad (10)$$

where $\mu_f = \varepsilon_n\varphi_f$ is the consumption coefficient of the first sheath in the path (I)–(II). It is not difficult to determine the velocity coefficients φ_{rm} and φ_{rf} because there are well known methods [18] used to obtain loss coefficients along the length ξ_l and at various obstacles ξ_r. The velocity distribution over the cross section has been studied, for example, by *Bird* et al. [17]. It is easy to prove that the Coriolis coefficient for a laminar flow of liquid in round- or square-shaped channels, determined by Eq. (3), are equal to 4/3 and 6/5, respectively. However, even for axialsymmetric flows it is difficult to calculate the pressure coefficient ξ_e, taking into account the transfer of kinetic energy via the border of flow separation, in order to calculate the velocity component φ_e by Eq. (7). Therefore, for engineering calculations of the parameters of the running-type chamber the dependence of φ_e on the ratio of average velocities of bordering flows has to be obtained experimentally.
It must be mentioned that the correctness of Eq. (9) is confirmed by the fact that the boundary conditions are satisfied: At $Q_f/Q_m = \infty$, the coefficient k tends to infinity. If the first sheath is absent ($Q_f = 0$; $\varphi_m = 1$, which is caused by absence of energy transfer between the flows) and if the section plane (I) is located above nozzle 4, the compression coefficient is equal to $1/\varepsilon_c$, but if this plane is located below the nozzle, then $k = 1/\chi$ (at $S_{p2} \le S_c$) and $k = 1/\varepsilon_c$ (at $S_{p2} > S_c$).

3 Experimental Results

The proposed technique has been used to design a running-type chamber with two sheaths (see Figure 1). To prevent the clogging of the running-type chamber openings with random large particles, the minimum diameter of the openings has been taken in excess of 200 μm. Thus, the diameter of capillary 1 is $2r_c$ = 217 μm ($S_c = 0.037$ mm^2), its length $l_c = 16$ mm, the pipe diameter was taken as $2r_{p2} = 512$ μm, i.e. $S_{p2} = 0{,}21$ mm^2 and $\chi = S_{p2}/S_c = 5.7 \gg 1$. Size $2r_{p1} = 6.5$ mm ($S_{p1} = 33.18$ mm^2) does not influence the chamber operation. The taper angle of nozzle 4 is 13°. The nozzle 4 and the capillary 1, which were chosen in accordance with reference data from *Bogomolov* [18], had the following parameters: $\varepsilon_n = 0.982$, $\varphi_{rf} = 0.965$, $\varepsilon_c = 1$ and $a_{m1} = 1$. The suspension being examined in the path (I)–(II) has no contact with the channel walls so that $\varphi_{rm} = 1$. The running-type chamber has been manufactured with due account of the obtained design parameters and in accordance with Figure 1.
For this chamber the dependence of the compression coefficient k on the ratio Q_f/Q_m of the flow rate of the sheath to that of the examined suspension has been found experimentally and is presented in Figure 4.
At $k > 4$ this dependence is linear. It confirms the character of the theoretical dependence of k on Q_f/Q_m according to Eqs. (9) and (10).
The experimental data (see Figure 4) allows one to determine the internal flow for the dependence of the velocity coefficient on V_{in}/V_{ext}, where V_{in} and V_{ext} are the average velocities of the internal and external coaxial flows at the path with the top value of the ratio V_{in}/V_{ext}. In this case it is necessary to take into consideration the following facts:

- the ratio of average velocities of the suspension being examined and of the first sheath V_m/V_f has the top value in the zone adjoining section I, because

$$\max\left(\left(\frac{V_m}{V_f}\right)_i\right) = \max\left(\frac{S_{p1}Q_m}{S_cQ_f}\right) = \frac{S_{p2}Q_m}{S_cQ_f}; \quad (11)$$

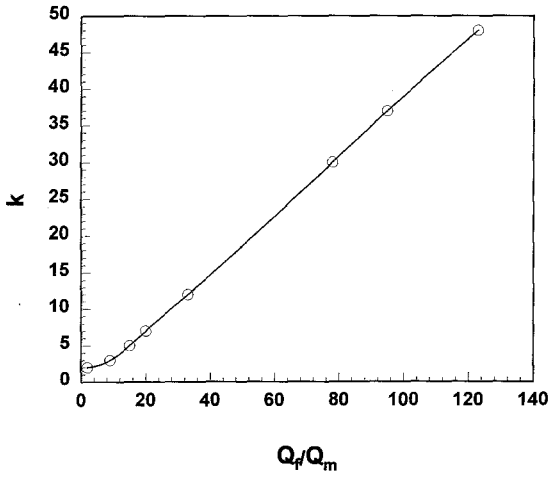

Fig. 4: Experimentally obtained dependence of the coefficient of hydrodynamic compression k on the ratio of the first sheath flow rate to the flow rate of the suspension being examined.

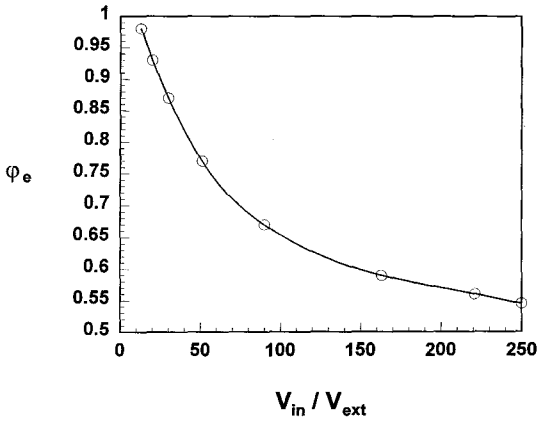

Fig. 5: Dependence of coefficient φ_e of the velocity of internal flow on the maximum ratio of the velocities of internal V_{in} and external V_{ext} coaxial flows.

- the component φ_{em} of the velocity coefficient of the examined flow approaches 1 at sufficiently large values of Q_f/Q_m, when V_m and V_f become comparable in accordance with Eq. (11), since $\varphi_e\ (V_{in}/V_{ext}) = 1$;
- the component of the velocity coefficient of the first sheath $\varphi_{ef} = \varphi_e\ (V_{in}/\ V_{ext} \to \infty)$, since for the first sheath the ratio of average velocities of the first and second "sheaths" V_f/V_s in the area of their common flow exceeds 400.

Indeed,

$$\frac{V_f}{V_s} \geq \frac{S_{pl}}{S_{p2}} \min\left(\frac{Q_f}{Q_s}\right) = \frac{S_{pl}}{4S_{p2}} = 400\ , \qquad (12)$$

because of the following factors:

- the cross-sectional area of the external chamber 5 has been chosen rather large ($S_{c5} = 320\ mm^2$) in order to reduce a probability of optical damage to the chamber walls, which are transparent to the laser beam, by random particles;
- the lowest value of Q_f/Q_s for this chamber type is 1/4.

With due account of the above and on the basis of the correlation of the experimental data (see Figure 4) with theoretical results according to Eqs. (5), (6) and (8), the dependence of the coefficient of internal flow velocity φ_e, which takes into consideration the transfer of kinetic energy via the border of separation to the external coaxial flow with lower energy, on the largest ratio of average velocities of the internal and external flows has been obtained and is presented in Figure 5.

At $V_{in}/V_{ext} \to \infty$, φ_e asymptotically approaches 0.5. Thus, as $V_{in}/V_{ext} > 400$ irrespective of the chamber operation mode, for the described chamber of running type $\varphi_{ef} \approx 0.5$ and with due account of the equation for φ_f similar to Eq. (5) $\mu_f = \varepsilon_n \varphi_f = 0.487$.

As an example of modelling the hydrodynamic focusing, we can show that for the purpose of focusing the diameter of a measured suspension jet sixfold ($2r_{m2} = 2r_c/6 \approx 36\ \mu m$) it is necessary to choose the ratio $Q_f/Q_m = 100$ (see Eq. (10)). Hence, if $P_1 - P_2 = 0.1$ bar then $Q_f \approx 4.7 \cdot 10^{-7}\ m^3/s$, $V_{f2} \approx 5$ m/s, $Q_m \approx 4.7 \cdot 10^{-9}\ m^3/s$ and $V_{m2} \approx 4.6$ m/s. It must be mentioned that the application of Eqs. (9) and (10), the dependence φ_e (Figure 5), and the well known methods of determining φ_r, ξ_r and ξ_l [18] for calculating the compression coefficient of the running-type chamber with other design parameters and also without the second sheath (when the common paths length of coaxial flow of bordering liquids is not over 20 mm) led to a divergence from the experimental data of less than 7%.

4 Conclusion

This work was carried out because of the necessity to reduce measurement errors of particle size laser analysers by using a running-type chamber with optimum design parameters. For this purpose the method of hydrodynamic theory has been used. Simple equations intended for designing running-type chambers, in which the trajectories of the examined particles are focused in relation to the centre of the analyser measurement zone, have been obtained. The focusing is provided by applying liquids of one or two buffer "sheaths". Experimental research has proved the correctness of the proposed technique for designing running-type chambers. The expediency of the application of these methods during the development of laser analysers with improved metrological characteristics has been demonstrated.

5 Acknowledgements

The author is grateful to the Alexander von Humboldt Foundation for its support of this work.

6 Symbols and Abbreviations

a	Coriolis coefficient for proper flow of liquid
d	particle diameter
g	acceleration due to gravity
h_j	distance from the jth plane of section to an arbitrarily selected horizontal plane
k	compression coefficient of the flow of suspension being examined in the measurement zone
P_j	pressure in the jth plane
Q	flow rate
r	radius
S	area
V	average velocity of the flow
γ	specific gravity of liquid
ε	flow compression coefficient
ξ	coefficient of energy losses of a liquid flow

μ consumption coefficient of proper flow accounting for energy losses
φ velocity coefficient of proper flow

Subscripts:

c, n, p for designation of physical parameters describing the capillary 1 (*c*), nozzle 6 (*n*), pipe 3 (*p*) (see Figure 1)
i for designation of the *i*th obstacle in the way of liquid flow
j for designation of the section of the *j*th path of the running-type chamber at which the average velocity of the proper flow does not change
m, f, s for designation of the suspension being examined (measured) (*m*) and flow of the first (*f*) and second (s) sheaths
e, l, r designation of energy transfer via the border of flow separation (*e*) and losses of energy for friction along the path of flow (*l*) and at obstacles (*r*)
in, ext for designation of velocities of internal and external coaxial flows

7 References

[1] *K. Leschonski:* Particle characterization: present state and possible future trends. Part. Charact. *3* (1986) 99–103.
[2] *J. Gebhart:* Response of single-particle optical counters to particles of irregular shape. Part. Part. Syst. Charact. *8* (1991) 40–47.
[3] *M. Bottlinger, H. Umhauer:* Single particle light scattering size analysis: qualification and elimination of the effect of particle shape and structure. Part. Part. Syst. Charact. *6* (1989) 100–109.
[4] *J. A. Steinkamp, M. J. Fulwyler, J. R. Coulter, R. D. Hiebert, J. L. Horney, P. F. Mullaney:* A new multiparameter separator for microscopic particles and biological cells. Rev. Sci. Instrum. *44* (1973) 1301–1310.
[5] *V. I. Ovod, V. Ya. Shlyuko, E. I. Moshkovskiy, A. B. Lyashenko:* A rapid method for determining the particle-size distribution of micropowders. Sov. Powder Metall. Metal Ceram. *23* (1984) 825–828 (in English).
[6] *V. I. Ovod, V. Ya. Shlyuko:* High-speed laser analyzer of microparticle size distribution. Sov. Powder Metall. Metal Ceram. *24* (1985) 505–509 (in English).
[7] *U. Manasse, Th. Wriedt, K. Bauckhage:* Phase-Doppler sizing of optically absorbing liquid droplets: comparison between Mie theory and experiment. Part. Part. Syst. Charact. *9* (1992) 176–185.
[8] *W. D. Bachalo, S. V. Sankar:* Analysis of the light scattering interferometry for spheres larger than the light wave-length. Proc. Fourth Int. Symp. on Applications of Laser Anemometry to Fluid Mechanics, Lisbon, Portugal, July 11–14, 1988, paper 1.8.
[9] *Y. Aizu, F. Durst, G. Gréhan, F. Onofri, T.-H. Xu:* PDA-system without Gaussian beam defects. Proc. Third Int. Congress on Optical Particle Sizing, Yokohama, August 23–26, 1993, 461–470.
[10] *J. A. Steinkamp:* Flow cytometry. Rev. Sci. Instrum. *5* (1984) 1375–1400.
[11] *H. S. Lee, S. K. Chae, B. Y. H. Liu:* Size characterization of liquid-borne particles by light scattering counters. Part. Part. Syst. Charact. *6* (1989) 93–99.
[12] United States Atomic Energy Commission, US Pat. 1380756 (1971).
[13] *G. C. Salzman, P. F. Mullaney* (United Energy Research and Development Administration), US Pat. 3946239 (1975).
[14] *V. Kachel:* Investigations into Coulter sizing of biological particles; theoretical background and instrumental improvements. Part. Charact. *3* (1986) 45–55.
[15] *B. Gransson:* Improved accuracy in the measurement of particle size distribution with a Coulter equipped with a hydrodynamically focused aperture. Part. Part. Syst. Charact. *7* (1990) 6–10.
[16] *H. G. Merkus, H. Liu, B. Scarlett:* Improved resolution and accuracy in electrical sensing zone particle counters through hydrodynamic focussing. Part. Part. Syst. Charact. *7* (1990) 11–15.
[17] *R. B. Bird, W. E. Stewart, E. N. Lightfoot:* Transport Phenomena. Wiley, New York 1960.
[18] *A. I. Bogomolov* (ed.): Examples of Hydraulic Calculations. Transport, Moscow 1977.